Accepted Manuscript

Biotransformation of copper oxide nanoparticles by the pathogenic fungus *Botrytis cinerea*

Eva Kovačec, Marjana Regvar, Johannes Teun van Elteren, Iztok Arčon, Tamás Papp, Darko Makovec, Katarina Vogel-Mikuš

PII: S0045-6535(17)30545-3

DOI: 10.1016/j.chemosphere.2017.04.022

Reference: CHEM 19079

To appear in: *ECSN*

Received Date: 25 January 2017

Revised Date: 3 April 2017

Accepted Date: 4 April 2017

Please cite this article as: Kovačec, E., Regvar, M., van Elteren, J.T., Arčon, I., Papp, Tamá., Makovec, D., Vogel-Mikuš, K., Biotransformation of copper oxide nanoparticles by the pathogenic fungus *Botrytis cinerea*, *Chemosphere* (2017), doi: 10.1016/j.chemosphere.2017.04.022.

Biotransformation of copper oxide nanoparticles by the pathogenic fungus *Botrytis cinerea*

Eva Kovačec[a], Marjana Regvar[a], Johannes Teun van Elteren[b], Iztok Arčon[c,e], Tamás Papp[d], Darko Makovec[e], and Katarina Vogel-Mikuš[a,e,*]

[a] Department of Biology, Biotechnical Faculty, University of Ljubljana, Jamnikarjeva 101, Ljubljana, Slovenia;

[b] National Institute of Chemistry, Hajdrihova 19, Ljubljana, Slovenia;

[c] University of Nova Gorica, Vipavska 13, Nova Gorica, Slovenia;

[d] MTA-SZTE Fungal Pathogenicity Mechanisms Research Group, 6726 Szeged, Kozep fasor 52., Hungary; [e] Jožef Stefan Institute, Jamova cesta 39, Ljubljana, Slovenia;

[*] Corresponding author:

Katarina Vogel-Mikuš;

katarina.vogelmikus@bf.uni-lj.si

tel +386132033416; fax +38612573390

Abstract

Two plant pathogenic fungi, *Botrytis cinerea* and *Alternaria alternata*, isolated from crop plants, were exposed to Cu in ionic (Cu^{2+}), microparticulate (MP, CuO) or nanoparticulate (NP, Cu or CuO) form, in solid and liquid culturing media in order to test fungal response and toxic effects of the mentioned compounds for the potential use as fungicides. *B. cinerea* has shown pronounced growth and lower levels of lipid peroxidation compared to *A. alternata*. Its higher resistance/ tolerance is attributed mainly to biotransformation of CuO and Cu NPs and CuO MPs into a blue compound at the fungal/ culturing media interface, recognized by Cu K-edge EXAFS analysis as Cu-oxalate complex. The pronounced activity of catechol-type siderophores and organic acid secretion in *B. cinerea* induce leaching and mobilization of Cu ions from the particles and their further complexation with extracellularly secreted oxalic acid. The ability of pathogenic fungus to biotransform CuO MPs and NPs hampers their use as fungicides. However the results show that *B. cinerea* has a potential to be used in degradation of Cu(O) nanoparticles in environment, copper extraction and purification techniques.

Keywords

Botrytis cinerea; copper; metal oxide nanoparticles; detoxification mechanisms; metal pollution, Cu-oxalate.

Abbreviations

ELM…experiment with liquid media

ESM…experiment with solid media

NPs…nanoparticles

44

45 **Highlights**

46 • *B cinerea* is more resistant/ tolerant to CuO and Cu NPs than *A. alternata*

47 • *B. cinerea* excretes oxalic acid and catechol-type siderophores

48 • *B. cinerea* is able to biotransform CuO and Cu NPs to Cu-oxalate

49 • CuO and Cu NPs may not be efficient in treating *B. cinerea* based plant diseases

50 • *B. cinerea* could be used for cleaning environment contaminated with CuO and Cu NPs

51

1 Introduction

In agricultural ecosystems many Cu compounds have been used for decades to suppress fungal and bacterial plant diseases (Komárek et al., 2010). Long-term exposure of pathogenic fungi and bacteria to Cu, however, has lead to development of Cu tolerance/ resistance, so more and more Cu needs to be applied for the same level of plant protection. Several tolerance mechanisms at intra- and extra-cellular levels have been demonstrated, from extracellular precipitation and complexation, binding to the cell wall components, to transport into the cell with intracellular detoxification (Cervantes and Gutierrez-Corona, 1994).

One of the most widespread fungal plant pathogens is *Alternaria alternata*, infecting over 380 plant species and considered to be Cu sensitive. Another important phytopathogenic fungus causing economic losses worldwide is *Botrytis cinerea*, recently classified among the top 10 fungal pathogens in molecular plant pathology (Dean et al., 2012). *B. cinerea* infects tomatoes by down-regulation of the plant gene for proteins with high similarity to a copper chaperone, relating copper homeostasis to plant defence responses (Company and González-Bosch, 2003). On the other hand, fungal Cu-containing proteins are required for the pathogenicity of *B. cinerea* (Saitoh et al., 2010)..

Currently, a need for novel strategies and new antimicrobial agents with broad-spectrum antimicrobial activity and an ideal ratio between solubility and stability is emerging (Ingle et al., 2014). Lowering the size of agent particles increases their solubility and activity, as well as toxicity. Thus, metallic nanoparticles (NPs) are widely explored as potential antimicrobials (Ingle et al., 2008). Different Cu particles are used in various technological applications such as micro-electromechanical systems, transistors, electrochemical cells, solar cells as well as fungicides and different types of coatings. Because of smaller size

and higher surface-to-volume ratio, CuO NPs are much more toxic than microparticles (MPs), despite their low solubility (Bodarenko et al., 2013). The data on Cu NP antifungal activity are scarce (Ingle et al., 2014). Micronized Cu was shown to be more efficient against wood-destroying fungi than conventional formulations, promising to become the major global wood protection agent (Civardi et al., 2015).

Once in the environment, NPs can act as an ecotoxicological hazard, undergoing biodegradation or bioaccumulation in the food chain (Keller et al., 2013) threatening to become the most difficult type of pollution to manage and control (Gao et al., 2013). Consequently, the uptake and accumulation of NPs by fungal biomass is receiving increasing attention since microbe-based technologies may provide alternative techniques for removal of NPs from polluted soils and waste waters. For example, Cu-tolerant filamentous fungi isolated from agricultural fields are applied in the cleaning of Cu-containing wastewaters (Zafar et al., 2007). A better understanding of the mechanisms allowing fungi to survive in the presence of high concentrations of metals and/ or NPs is therefore of both environmental and economic significance.

The aim of this work was to study the interactions of two phytopathogenic fungi, *A. alternata* and *B. cinerea*, with Cu in ionic (Cu^{2+}), microparticulate (CuO) or nanoparticulate (Cu or CuO) form in order to assess the fungal response and toxicity. Biomass and the level of lipid peroxidation were used as indicators for the resistance/ tolerance to Cu compounds. In addition, the amounts of exuding siderophores and organic acids were determined. Cu distribution across the medium/ fungal interface was followed by X-ray fluorescence spectrometry (XRF) for mycelium grown on solid medium and laser ablation inductively coupled plasma mass spectroscopy (LA-ICP-MS) for mycelium grown in liquid

99 medium. Cu chemical state in the newly formed extracellular blue compound was
100 characterized by Cu K-edge EXAFS (Extended X-ray Absorption Fine Structure).
101
102 **2 Materials and methods**
103 **2.1 Experimental design**
104 This study included two experimental approaches: experiments with solid (ESM) and liquid
105 media (ELM). Liquid media were used to estimate the fungal growth performance, organic
106 acid exudation, MDA levels and Cu profile patterns by LA-ICPMS. Solid media that are
107 more close to the fungal natural environment were used to assess the appearance of the
108 fungi. The blue compound for Cu-K EXAFS analysis was also isolated from solid media.
109 The growing medium, Melin-Norkrans-Marx (MNM) (Marx, 1969), was supplemented with
110 various Cu compounds: CuO MPs (Sigma Aldrich, Germany), CuO NPs (Aldrich chemistry,
111 USA; particles size <50 nm), Cu NPs (Aldrich chemistry, USA; particles size 60-80 nm)
112 and $CuSO_4 \cdot 5H_2O$ (Sigma Aldrich, Germany). The tested fungal strains belonged to
113 *Alternaria alternata* (GenBank Acc. No. KP985749) and *Botrytis cinerea* (GenBank Acc.
114 No. KP985745), isolated from buckwheat grains and deposited in the fungal bank of the
115 Plant physiology Laboratory, Biotechnical Faculty, University of Ljubljana, Slovenia
116 (Kovačec et al., 2016).
117 In ESM, 50 mg of Cu and CuO (0.8 mg cm^{-2}) in different formulations suspended in ethanol
118 (EtOH), and $CuSO_4 \cdot 5H_2O$ (only 10% of the given amount of 50 mg) in MilliQ water was
119 evenly spread on the surface of 30 ml solid MNM medium in Petri-dishes. Controls were
120 covered with pure EtOH. After EtOH evaporation an agar plug (10 mm), obtained from the
121 actively growing edge of the 1-week old mycelia, was inoculated in the center of the Petri-
122 dish. The cultures were kept in dark at room temperature (24 ℃) and photographed

weekly till the 12th week. The experiment was repeated three times, with 10 replicates and served for Cu profiling across Petri-dishes with XRF and Cu speciation analyses. In addition, siderophore excretion was also studied on solid medium as described below.

In ELM one tested unit represented 100 ml of MNM liquid medium, supplemented with 166 mg of Cu in different formulations, in order to maintain the same Cu level as in ESM. In the $CuSO_4 \cdot 5H_2O$ treatment, however, only 1 and 10% of the dose were applied due to extreme toxicity of free Cu ions. Every flask was inoculated with one agar plug (6 mm) and kept at 24 ℃ in the dark on an orbital shaker at 175 rpm. After two weeks the fresh and dry fungal biomass was assessed after freeze-drying. Part of the mycelia was used for determination of the lipid peroxidation level and analysis of the Cu distribution by LA-ICP-MS (see Sections 2.3 and 2.5). In the filtered medium pH and organic acids were determined (see Section 2.6). Each treatment had five replicates and each experiment was performed in triplicate.

In order to study the general fungal tolerance/ resistance mechanisms to Cu, the growth of both fungi was also tested in MNM liquid media with different Cu ion concentrations (0.2, 0.4, 0.6, 0.8, 1, 1.25, 1.5, 1.75, 2, 2.5, 5, 7.5 and 10% of the Cu amount of 166 mg/ 100 ml set in ELM and supplied as $CuSO_4 \cdot 5H_2O$.

2.2 Characterization of copper particles and leaching of copper ion

Size, shape and surface chemical composition of purchased CuO MPs, CuO NPs and Cu NPs were investigated by transmission electron microscope coupled by energy-dispersive X-ray spectroscopy and electron diffraction (TEM JEOL 2010F with EDX detector Oxford Instruments ISIS300). The zeta potential of aqueous suspensions (prepared with MiliQ water) was determined (ZetaPALS, Brookhaven Instruments Corporation, USA) and

impurities in pressed pellets of chemical powders were determined by XRF (Nečemer et al., 2008).

The test of leaching of Cu ions from different Cu particles was performed in ELM by a chemical method for determination of Cu ions in solution, based on formation of blue colored complexes between copper and ammonium ions (Prenesti et al., 2002).

2.3 Lipid peroxidation

The quantity of malondialdehyde (MDA), as indicator for the level of lipid peroxidation of membranes, was determined in fresh mycelia from ELM by the TBA spectrophotometric method (Hodges et al., 1999).

2.4 Copper distribution across growing plate

Concentration of Cu across inoculated Petri-dishes from ESM was determined by a portable XRF spectrometer, Peduzo P01 (Jozef Stefan Institute, Slovenia) with Rh X-ray tube and SDD (Amptek, USA) detector. The tube energy was set to 35 keV. The beam was collimated to 5 mm and the energy resolution was 140 eV at 5.6 keV. The quantitative analysis was performed by the Quantitative X-ray analysis system software package developed in Lab View. The results were validated using standard reference material (tomato leaves NIST SRM 1573a) (Nečemer et al., 2008).

2.5 Copper distribution in mycelia cross sections from liquid media

The freeze-dried hand cuttings of mycelia from ELM were line scanned by LA-ICP-MS (Debeljak et al., 2013) to obtain information on Cu distribution across mycelia. A 193 nm ArF* excimer laser ablation system (Analyte G2, Teledyne Photon Machines Inc., Boze-

man, MT) interfaced with a quadrupole ICP-MS instrument (Agilent 7900, Agilent Technologies, Santa Clara, CA) was used in line scanning mode using the following operational conditions: laser energy density, 0.75 J cm^{-2}; repetition rate 10 Hz; laser beam diameter, 20 µm (round mask); scanning speed, 40 µm s^{-1}; acquisition time, 0.5 s. Ablation took place in a HelEx 2-volume cell, and helium (carrier glass flow rate, cup = 0.5 l min^{-1}; cell = 0.3 l min^{-1}) was used to transport the ablated material from the ablation cell to the inductively coupled plasma (ICP); argon (0.8 l min^{-1}) was added as a makeup gas before the torch of the ICP. The mass spectrometer was deployed in time-resolved analysis mode, measuring one point per mass and acquiring the masses of interest (^{63}Cu). Measurement of the back- ground gases (He/Ar mixture) provided a gas blank signal for the measured masses.

2.6 Siderophores and organic acid production

Fungi were tested for siderophores production on solid Chrome azurol sulphonate (CAS) medium (Schwyn and Neilands, 1987).

High performance liquid chromatography (HPLC) equipped with a UV-VIS detector (SPD-10Avp, Shimadzu), Agilent Hi-Plex Ligand Exchange column (Agilent Technologies) and column oven (CTO-10ASvp, Shimadzu) to heat the column to 70 ℃, was used to determine the organic acid concentrations in media from ELM. Aliquots of 10 µl of the filtrates were injected and 2 mM H_2SO_4 was used as a mobile phase. The retention time of each signal was recorded at a wavelength of 210 nm and 240 nm. Chromatograms were compared to 11 organic acid references of acetic, ascorbic, citric, fumaric, itaconic, levulinic, maleic, malic, oxalic, succinic and gluconic acid, where values were expressed as organic acid mg g^{-1} fungal DW per day.

2.7 Copper speciation and ligand environment

Copper K-edge EXAFS analysis was used to directly probe the chemical state of Cu in the blue-colored spots at the fungal/culturing medium interface. Samples were freeze-dried and packed between 2 layers of 2.5 micron mylar foil and fixed on Al holders. The Cu K-edge EXAFS spectra were measured in transmission detection mode at the BM23 beamline of the European Synchrotron Radiation Facility (ESRF, Grenoble, France) (Vogel-Mikuš et al., 2010). The beamline was equipped with a Si 111 two-crystal monochromator with about 1 eV resolution at 9 keV. The absorption spectra were measured within the interval [−250 eV to 1000 eV] relative to the Cu K-edge (8979 eV). Samples were inserted between the first and the second ionization detectors, and a 7 micron thick Cu metal was placed between the second and the third ionization detector to establish exact energy calibration. In the absorption edge region, equidistant energy steps of 0.5 eV were used, while for the EXAFS region from 50 eV to 1000 eV above the absorption edge, equidistant k-steps ($\Delta k \approx 0.03$ Å^{-1}) were adopted, with an integration time of 1 s/step. To obtain a detailed structural information on Cu surrounding a quantitative EXAFS analysis was performed with the IFEFFIT program package (Ravel and Newville, 2005), where EXAFS model is constructed with FEFF program package (Rehr et al., 1992), based on Cu-oxalate XRD crystal structure data (space group P 21/c, lattice constants: a=5.9569 Å, b=5.5528 Å, c=5.1247 Å, $\alpha=90^{o}$, $\beta=115.177^{o}$, $\gamma = 90^{o}$) (Christensen et al., 2014). Only the contributions of the first four coordination shells in the R range from 1.0 Å to 3.4 Å were analyzed.

2.8 Statistical analyses

The data were first tested for normal distribution (XLSTAT 2014.5.03. Addinsoft). Analyses of variance (ANOVA) with the accompanied Tukey Post-Hoc test were performed using Statistica software (Statsoft 8).

3 Results and Discussion

3.1 Characterization of copper particles

Characterization of Cu particles by TEM imaging revealed that individual nanoparticles were larger than specified by the producer (MPs CuO 623 ±45 nm; NPs CuO 48 ±3 nm; NPs Cu 101 ±5 nm), as already reported (Buffet et al., 2011). CuO MPs are less spherical and bigger than CuO and Cu NPs (Fig. A) (Dimkpa et al., 2012). The isoelectric point (IEP) of metal oxides in aqueous suspensions is usually pH-neutral, but in our case the IEPs of CuO MPs and CuO/ Cu NPs were 10 and 8, respectively. The EDX analyses of Cu NPs showed the presence of oxygen, suggesting the presence of oxides on the surface, which can also explain the same IEP as measured for CuO NPs (Neal, 2008).

Zeta potential measurements serve as predictor of toxicity of NPs with low solubility; however, the relationship between IEP and NPs-cell interaction is still not fully understood (Dimkpa et al., 2012). Differing IEP values may be mostly due to impurities (Gajewicz et al., 2015). XRF showed that Cu NPs contain traces of Sn, Ca (<1%) and Fe (<0.1%), CuO NPs traces of Sn, Ca (<1%), Cr, Mn (<0.05%), Fe (<0.1%), Ni (<0.05%) and CuO MPs traces of Sn, Ca (<1%), Fe (<0.1%) and Ni (<0.05%).

3.2 Biomass and stress parameters

In order to estimate the levels of stress and tolerance/ resistance, biomass and MDA levels were determined at the end of each experiment. *Botrytis cinerea* showed increased growth

at lower ionic Cu concentrations in comparison to the control (up to 178%), while in *A. alternata* the growth was suppressed (max 92%) (Fig. B). Increased growth in *B. cinerea* thus indicates a preference of smaller amount of Cu in ionic form and/ or dependence thereon. *Botrytis cinerea* was shown to develop resistance/ tolerance to Cu under laboratory conditions (Parry and Wood, 1958). The organism that are resistant/ tolerant to metals possess very efficient mechanisms for metal detoxification, therefore they may develop an increased need for the mentioned metals and may grow better at moderately higher concentrations, as in the case of metal hyperaccumulating plants (Koren et al., 2013). A significant persistence was reported even in environments where Cu-based fungicides have been applied (Komárek et al., 2010). In our case the development of Cu tolerance/ resistance may be attributed to agricultural management (use of pesticides) of the fields from which the fungus was isolated.

The average biomass in all treatments with different Cu formulations decreased for 55% in *A. alternata* and increased for 56% for *B. cinerea* in comparison to controls (Fig. 1b). *Botrytis cinerea* is thus more tolerant/ resistant than *A. alternata* (Ouda, 2014). With the latter, the toxicity of the treatments, resulting in higher lipid peroxidation, follows the expected order: $CuSO_4 \cdot 5H_2O$ (1%) < CuO MPs < CuO NPs < Cu NPs < $CuSO_4 \cdot 5H_2O$ (10%) (Fig. 1b). Compared to the controls the biomass of *B. cinerea* increased for 147 and 207% in treatment with CuO MPs and CuO NPs, respectively. Reported toxicological studies on many different organisms showed higher toxicity of CuO NPs in comparison to CuO MPs (Bodarenko et al., 2013), but interestingly this is not the case for *B. cinerea*. Furthermore, significantly lower water content in *A. alternata* mycelia treated with CuO MPs and CuO NPs, as well as in *B. cinerea* treated with Cu NPs (Fig. 1a), suggests the adherence of particles to the fungal cell walls. The immobilization of the (nano)particles, as

well as leached Cu ions on the surface of the cells reduces their bioavailability and toxicity, indicating that cell wall composition may play an important role in detoxification (Judet-Correia et al., 2011).

Concentrations of MDA reflect the levels of oxidative stress in treated fungi, since an increased MDA level is an indicator of cell membrane lipid peroxidation and in essence a measure of membrane damage. The level of stress in ELM, as indicated by MDA was, with the exception of CuO MPs, lower in *B. cinerea* than in *A. alternata*. The lowest concentration of MDA was found in *B. cinerea* grown in control media, while the highest MDA levels were recorded in *A. alternata* grown in Cu NPs (Fig. 1c), together with significantly suppressed fungal growth (Fig 1b). Generally, NPs can cause cell membrane damage and loss of its integrity via specific or nonspecific interactions, such as oxidation of membrane proteins and ROS generation, or membrane wrapping with the nanoparticles resulting in malfunction of vital cellular processes (Nel et al., 2009). Leaching of Cu ions may also contribute to toxicity.

3.3 Appearance of treated fungi and copper distribution

The Cu distribution across mycelia grown in Petri dishes (ESM) and in ELM depended on the treatment as well as the fungal species (Figs. 2, 3). In the 12-week period the *B. cinerea* mycelia normally covered a whole Petri-dish, while the applied $CuSO_4 \cdot 5H_2O$ completely inhibited fungal growth (Fig. 2). With the black Cu particles tested in this study, evenly distributed across the Petri-dish, and with mycelia growing from the center towards the edge, a blue-colored compound was appearing at the mycelia/ medium interface followed by a transparent zone: the picture was confirmed by XRF as a sharp Cu peak followed by a clear decline (Fig. 2). The biotransformation of black Cu compounds to the

blue-colored compound was prominent on Petri-dishes with *B. cinerea*, while totally absent in *A. alternata*.

LA-ICPMS results presented in Fig. 3 reveal Cu profile patterns in particular fungal - Cu formulation combinations. In mycelia from ELM of both fungal species grown in the presence of $CuSO_4 \cdot 5H_2O$, LA-ICP-MS revealed a similar distribution, with Cu located in older mycelia (Fig. 3). In *A. alternata* grown in the presence of particles, Cu was found in younger mycelia, and similarly, in *B. cinerea* grown in Cu NPs media. This is in line with NPs remaining firmly attached to the cell walls, similarly as in bacteria, even after washing (Applerot et al., 2009). Cu and CuO NPs did not penetrate in older parts of mycelium indicating very strong immobilization of NPs by fungal hyphae. In *B. cinerea*, treated with CuO MPs or NPs, Cu was found localized respectively in the center (old mycelia) and in a thin zone between the young and old mycelia. The color of the zone was not black, confirming the biotransformation of the particles as in ESM.

3.4 Cu leaching, siderophores, and organic acid production

In order to further elucidate the mechanisms of CuO biotransformation, leaching of Cu^{2+} ions from NPs and MPs was examined, together with the contents of excreted siderophores and organic acids.

Ion leaching is one of the proposed mechanisms for the toxicity of metal oxide NPs, next to the mechanisms involving redox properties of metal-oxide surfaces and the “Troian horse” effect, where NPs are internalized and dissolved intracellularly (Gajewicz et al., 2015). In our experiments, the formation of Cu^{2+} ions in ELM through CuO leaching was higher in media inoculated with *B. cinerea* (average 11.4%) than with *A. alternata* (average 5.2%) (Table 1). As reported by many authors, leaching of Cu^{2+} ions from the particles occurs to

some degree naturally and depends on the size of the particles (Bodarenko et al., 2013; Ding et al., 2013). The leaching from CuO NPs proved to be also pH dependent (Ding et al., 2013).

Both fungi showed ability to produce siderophores on CAS agar (Fig. 4a, b); *A. alternata* in the form of yellow halos (224 ±13 mm^2) and *B. cinerea* in the form of purple halos (1353 ±45 mm^2) surrounding the mycelia. *Alternaria alternata* synthesized lower amount of siderophores than *B. cinerea*, according to the color change, they were, respectively, of hydroxamate and catecholate type (Pérez-Miranda et al., 2007). Both are able to form strong chelates with metals and can directly affect their relative availability. Normally the divalent cations possess lower affinity for siderophore binding than trivalent cations; nevertheless, it is well known that siderophores can bind Cu^{2+} (Koh and Henderson, 2015). Excretion of catecholate type of siderophores in *B. cinerea* may, according to our results, contribute to the leaching of Cu^{2+} from CuO; however, the formation of blue-colored spots indicates a rapid chelation and detoxification of the leached Cu ions.

Among organic acids, the amount of oxalic acid varied the most between the both fungal species. In ELM its production was much higher in *B. cinerea* than in *A. alternata*, with average values of 4540 and 204 mg g^{-1} DW day^{-1}, respectively. Oxalic acid concentrations were lower in media of *B. cinerea* supplemented with particles, and higher in media with $CuSO_4 \cdot 5H_2O$ (10%) when compared to the controls (Table 1). In media of *A. alternata*, the production of oxalic acid was induced with CuO NPs and Cu NPs, while there was no induction seen in the control, CuO MPs and $CuSO_4 \cdot 5H_2O$ media. The 10% $CuSO_4 \cdot 5H_2O$ media totally depressed *A. alternata* growth and was too toxic to stimulate oxalic acid production, while in the control and 1% $CuSO_4 \cdot 5H_2O$ media the Cu concentrations were probably too low. It was already shown that *B. cinerea* produces oxalate *in vitro* as well as

in planta (Gadd et al., 2014) and that oxalic acid is responsible for biotransformation of minerals into Cd-, Cu- and Zn-oxalates, by pH-induced speciation changes or through direct complexation (Gadd et al., 2014). The pH values of media at the end of the experiment showed significant differences between the treatments (Table 1). The lowest values were seen in both fungi for the control media and the media supplemented with $CuSO_4 \cdot 5H_2O$ (1%), followed by CuO MPs < CuO NPs < $CuSO_4 \cdot 5H_2O$ (10%) < Cu NPs. Gluconic, fumaric and maleic acid were present in almost all media in low concentrations, while acetic acid was detected in all *B. cinerea* treatments and in treatment of *A. alternata* with $CuSO_4 \cdot 5H_2O$ (1%) media. Via simple *in vitro* experiments we have shown that oxalic acid in solution is sufficient to leach CuO MPs and CuO NPs and complex Cu^{2+} ions to pale blue Cu-oxalate (Fig. C), similar in color as seen in ESM.

3.5 Copper speciation and ligand environment

The chemical state of Cu cations in the blue-colored spots at the fungal/culturing medium interface was determined by Cu K-edge EXAFS, providing direct information on the local structure of Cu atoms in the sample (number and species of neighbour atoms around Cu, their distance from the Cu atom, and the thermal or structural disorder of their positions). The EXAFS model comprised six oxygen atoms in the first coordination shell, four at a shorter distance of 1.93 Å and two at longer distance 2.46 Å, and three shells of carbon neighbors, two at 2.67 Å, two at 2.68 Å and two at 3.34 Å, Two variable parameters for each shell of neighbors were introduced in the model: the distance (R) and the Debye-Waller factor (σ^2). In addition, a common shift of energy origin ΔE_o is also allowed to vary. The shell coordination numbers (N) were kept fixed at the crystallographic values. The Cu-oxalate spectrum was used to calibrate the model. An excellent fit was obtained in the k

range of 3 $Å^{-1}$ to 14 $Å^{-1}$ and the R range of 1 to 3.0 Å (Fig. 5). The same model fitted very well the EXAFS spectrum of the blue Cu complex in the same R and k range. In both cases a best fit was obtained with ΔE_o of 8(2) eV and the fixed amplitude reduction factor S_o^2 of 0.98. The best fit values of structural parameters are listed in Table 2. The quality-of-fit parameter (R-factor) is 0.005 for oxalate and 0.009 for the blue complex spectrum. The results of Cu K-edge EXAFS analysis therefore clearly indicate that the blue compound formed by *B. cinerea*, when exposed to CuO NPs, is Cu-oxalate.

The oxygen ligands play a major role in metal coordination within the fungal biomass during the accumulation of differently mobilized toxic metals (Fomina et al., 2005). It is known that oxalic acid can directly bind Cu (Gadd et al., 2014), however, sometimes the production of oxalic acid does not seem to be the only factor controlling Cu tolerance/resistance. In our case the amount of Cu-oxalate increased with the amount of Cu supplemented into media, and the percentage of Cu leaching correlated with the amount of exuded oxalic acid in *B. cinerea* (r=0.69, $p<0.05$). We can therefore conclude that oxalic acid seems to play a dominant role in the biotransformation of Cu and CuO NPs and CuO MPs into Cu-oxalate.

4 Conclusions

Many authors have reported that *Botrytis cinerea* pathogenicity is related to the overproduction of oxalic acid, but to our knowledge this is the first evidence of *B. cinerea* to biotransform Cu and CuO NPs and CuO MPs to Cu-oxalate. In *B. cinerea* the prominent excretion of oxalic acid, possibly together with excretion of catechol-type siderophores induces leaching of Cu^{2+} ions from the particles that is followed by complexation to extracellularly secreted oxalic acid. Our finding provides evidence that nano-based CuO

preservatives and fungicides may not be efficient for suppression of *B. cinerea* related plant diseases. Furthermore, the results indicate that *B. cinerea* has the potential to be used in degradation of Cu(O) nanoparticles in environment, copper extraction and purification techniques.

Acknowledgments

The authors wish to thank Szekeres A. (SZTE) for his valuable suggestions regarding HPLC analyses and to Bencsik O. (SZTE), Nyilasi I. (SZTE) from University of Szeged and Murn T. (UL) for their technical assistance. Kump P. (IJS) is acknowledged for help in XRF analysis and prof. Kodre A. is acknowledged for language revision of the manuscript. Study was financed by the Slovenian Research Agency programmes (P1-0212, P1-0112 and P3-0395) and the IAEA framework of coordinated research projects RC 16796 (CSI, Katarina Vogel-Mikuš). The European Synchrotron Radiation Facility (ESRF), Grenoble, France, is acknowledged for provision of synchrotron radiation facilities at beamline BM23 (projects LS-2209 and LS- 2275). The authors are grateful to ESRF staff Parakhonskiy G., Iadecola A. and Mathon O. for assistance in using beamline BM23.

References

Applerot, B.G., Lipovsky, A., Dror, R., Perkas, N., Nitzan, Y., Lubart, R., Gedanken, A., 2009. Enhanced antibacterial activity of nanocrystalline ZnO due to increased ROS-mediated cell injury. Adv. Funct. Mater. 19, 842–852.

Bodarenko, O., Juganson, K., Ivask, A., Kasemets, K., Mortimer, M., Kahru, A., 2013. Toxicity of Ag, CuO and ZnO nanoparticles to selected environmentally relevant test organisms and mammalian cells in vitro: a critical review. Arch. Toxicol. 87, 1181–1200.

Buffet, P.E., Fossi, O., Pan, J.F., Berhanu, D., Herrenknecht, C., Poirier, L., Amiard-Triquet, C., Amiard, J.C., Bérard, J.B., Risso, C., Guibbolini, M., Roméo, M., Reip, P., Valsami-Jones, E., Mouneyrac, C., 2011. Behavioural and biochemical responses of two marine invertebrates *Scrobicularia plana* and *Hediste diversicolor* to copper oxide nanoparticles. Chemosphere 84, 166–174.

Cervantes, C., Gutierrez-Corona, F., 1994. Cooper resistance mechanisms in bacteria and fungi. FEMS Microbiol. Rev. 14, 121–137.

Christensen, A.N., Lebech, B., Andersen, N.H., Grivel, J.-C., 2014. The crystal structure of paramagnetic copper(ii) oxalate (CuC_2O_4): formation and thermal decomposition of randomly stacked anisotropic nano-sized crystallites. Dalt. Trans. 43, 16754–16768.

Civardi, C., Schwarze, F.W.M.R., Wick, P., 2015. Micronized copper wood preservatives: an efficiency and potential health risk assessment for copper-based nanoparticles. Environ. Pollut. 200, 126–132.

Company, P., González-Bosch, C., 2003. Identification of a copper chaperone from tomato fruits infected with *Botrytis cinerea* by differential display. Biochem. Biophys. Res. Commun. 304, 825–830.

427 Dean, R., Van Kan, J. A. L., Pretorius, Z. A., Hammond-Kosack, K.E., Di Pietro, A.,
428 Spanu, P.D., Rudd, J.J., Dickman, M., Kahmann, R., Ellis, J., Foster, G.D., 2012. The
429 Top 10 fungal pathogens in molecular plant pathology. Mol. Plant Pathol. 13, 414–
430 430.
431 Debeljak M., van Elteren, J.T., Vogel-Mikuš, K., 2013. Development of a 2D laser ablation
432 inductively coupled plasma mass spectrometry mapping procedure for mercury in
433 maize (*Zea mays* L.) root cross-sections. Anal. Chim. Acta 787, 155–162.
434 Dimkpa, C.O., Mclean, J.E., Britt, D.W., Anderson, A.J., 2012. CuO and ZnO nanoparticles
435 differently affect the secretion of fluorescent siderophores in the beneficial root
436 colonizer, *Pseudomonas chlororaphis* O6. Nanotoxicology 6, 635–642.
437 Ding, X., Meneses, M.B., Albukhari, S.M., Richter, D.L., Matuana, L.M., Heiden, P.A.,
438 2013. Comparing leaching of different copper oxide nanoparticles and ammoniacal
439 copper calt from wood. Macromol. Mater. Eng. 298, 1335–1343.
440 Fomina, M.A., Alexander, I.J., Colpaert, J. V, Gadd, G.M., 2005. Solubilization of toxic
441 metal minerals and metal tolerance of mycorrhizal fungi. Soil Biol. Biochem. 37, 851–
442 866.
443 Gadd, G.M., Bahri-Esfahani, J., Li, Q., Rhee, Y.J., Wei, Z., Fomina, M., Liang, X., 2014.
444 Oxalate production by fungi: significance in geomycology, biodeterioration and
445 bioremediation. Fungal Biol. Rev. 28, 36–55.
446 Gajewicz, A., Schaeublin, N., Rasulev, B., Hussain, S., Leszczynska, D., Puzyn, T.,
447 Leszczynski, J., 2015. Towards understanding mechanisms governing cytotoxicity of
448 metal oxides nanoparticles: Hints from nano-QSAR studies. Nanotoxicology 9, 313–
449 325.
450 Gao, Y., Luo, Z., He, N., Wang, M.K., 2013. Metallic nanoparticle production and

consumption in China between 2000 and 2010 and associative aquatic environmental risk assessment. J. Nanoparticle Res. 15, 1681–1689.

Hodges, D.M., DeLong, J.M., Forney, C.F., Prange, R.K., 1999. Improving the thiobarbituric acid-reactive-substances assay for estimating lipid peroxidation in plant tissues containing anthocyanin and other interfering compounds. Planta 207, 604–611.

Ingle, A., Gade, A., Pierrat, S., Sönnichsen, C., Rai, M., 2008. Mycosynthesis of silver nanoparticles using the fungus *Fusarium acuminatum* and its activity against some human pathogenic bacteria. Curr. Nanosci. 4, 141–144.

Ingle, A.P., Duran, N., Rai, M., 2014. Bioactivity, mechanism of action, and cytotoxicity of copper-based nanoparticles: a review. Appl. Microbiol. Biotechnol. 98, 1001–1009.

Judet-Correia, D., Charpentier, C., Bensoussan, M., Dantigny, P., 2011. Modelling the inhibitory effect of copper sulfate on the growth of *Penicillium expansum* and *Botrytis cinerea*. Lett. Appl. Microbiol. 53, 558–564.

Keller, A.A., McFerran, S., Lazareva, A., Suh, S., 2013. Global life cycle releases of engineered nanomaterials. J. Nanoparticle Res. 15, 1692–1708.

Koh, E.I., Henderson, J.P., 2015. Copper-binding siderophores at the host-pathogen interface. J. Biol. Chem. 290, 18967–18974.

Komárek, M., Čadkova, E., Chrastný, V., Bordas, F., Bollinger, J.C., 2010. Contamination of vineyard soils with fungicides: a review of environmental and toxicological aspects. Environ. Int. 36, 138–151.

Koren, Š., Arčon, I., Kump, P., Nečemer, M., Vogel-Mikuš, K., 2013. Influence of $CdCl_2$ and $CdSO_4$ supplementation on Cd distribution and ligand environment in leaves of the Cd hyperaccumulator *Noccaea* (*Thlaspi*) *praecox*. Plant Soil.

475 Kovačec, E., Likar, M., Regvar, M., 2016. Temporal changes in fungal communities from
476 buckwheat seeds and their effects on seed germination and seedling secondary
477 metabolism. Fungal Biol. 120, 666–678.
478 Marx, D.H., 1969. The influence of ectotrophic mycorrhizal fungi on the resistance of pine
479 roots to pathogenic infections. I. Antagonism of mycorrhizal fungi to root pathogenic
480 fungi and soil bacteria. Phytopathology 59, 153-163.
481 Neal, A.L., 2008. What can be inferred from bacterium-nanoparticle interactions about the
482 potential consequences of environmental exposure to nanoparticles? Ecotoxicology
483 17, 362–371.
484 Nečemer, M., Kump, P., Ščančar, J., Jaćimović, R., Simčič, J., Pelicon, P., Budnar, M.,
485 Jeran, Z., Pongrac, P., Regvar, M., Vogel-Mikuš, K., 2008. Application of X-ray
486 fluorescence analytical techniques in phytoremediation and plant biology studies.
487 Spectrochim. Acta Part B At. Spectrosc. 63, 1240–1247.
488 Nel, A.E., Mädler, L., Velegol, D., Xia, T., Hoek, E.M. V, Somasundaran, P., Klaessig, F.,
489 Castranova, V., Thompson, M., 2009. Understanding biophysicochemical interactions
490 at the nano–bio interface. Nat. Mater. 8, 543–557.
491 Ouda, S.M., 2014. Antifungal activity of silver and copper nanoparticles on two plant
492 pathogens, Alternaria alternata and *Botrytis cinerea*. Reasearch J. Microbiol. 9, 34–42.
493 Parry, K.E., Wood, K.S., 1958. The adaptation of fungi to fungicides: adaptation to copper
494 and mercury salts. Ann. Appl. Biol. 46, 446–456.
495 Pérez-Miranda, S., Cabirol, N., George-Téllez, R., Zamudio-Rivera, L.S., Fernández, F.J.,
496 2007. O-CAS, a fast and universal method for siderophore detection. J. Microbiol.
497 Methods 70, 127–131.
498 Prenesti, E., Daniele, P.G., Toso, S., 2002. Visible spectrophotometric determination of

499 metal ions: the influence of structure on molar absorptivity value of copper (II)
500 complexes in aqueous solution. Anal. Chim. Acta 459, 323–336.
501 Ravel, B., Newville, M., 2005. ATHENA, ARTEMIS, HEPHAESTUS: data analysis for X-ray
502 absorption spectroscopy using IFEFFIT. J. Synchrotron Radiat. 12, 537–41.
503 Rehr, J.J., Albers, R.C., Zabinsky, S.I., 1992. High-order multiple-scattering calculations of
504 x-ray-absorption fine structure. Phys. Rev. Lett. 69, 3397–3400.
505 Saitoh, Y., Izumitsu, K., Morita, A., Tanaka, C., 2010. A copper-transporting ATPase
506 BcCCC2 is necessary for pathogenicity of *Botrytis cinerea*. Mol. Genet. Genomics
507 284, 33–43.
508 Schwyn, B., Neilands, J.B., 1987. Universal chemical assay for the detection and
509 determination of siderophores. Anal. Biochem. 160, 47–56.
510 Vogel-Mikuš, K., Arčon, I., Kodre, A., 2010. Complexation of cadmium in seeds and
511 vegetative tissues of the cadmium hyperaccumulator *Thlaspi praecox* as studied by X-
512 ray absorption spectroscopy. Plant Soil 331, 439–451.
513 Zafar, S., Aqil, F., Ahmad, I., 2007. Metal tolerance and biosorption potential of filamentous
514 fungi isolated from metal contaminated agricultural soil. Bioresour. Technol. 98, 2557–
515 2561.
516

517 **Table 1. Oxalic acid production by fungi, media pH and % of Cu^{2+} leaching of CuO-**

518 **MPs, CuO-NPs and Cu-NPs.** Data are means ±SE (n=5). Different letters next to the

519 values represent statistically significant differences (Tukey test, performed for both fungal

520 species together; *p<0.05*); nd = not determined.

	Oxalic acid (mg g^{-1} DW day^{-1})		**pH**		**Leaching (%)**	
Treatment	*A. alternata*	*B. cinerea*	*A. alternata*	*B. cinerea*	*A. alternata*	*B.cinerea*
control	0 ±0 **a**	5610 ±458 **b**	3.3 ±0 **a**	3.3 ±0.1 **a**	nd	nd
$CuSO_4 \cdot 5H_2O$ (1%)	0 ±0 **a**	7040 ±1260 **bc**	3.2 ±0 **a**	3.1 ±0.2 **a**	nd	nd
CuO-MPs	0 ±0 **a**	1420 ±123 **a**	4.4 ±0 **bc**	4.1 ±0.2 **b**	3.68 ±1.44 **a**	9.7 ±0.88 **bc**
CuO-NPs	105 ±44 **a**	1200 ±235 **a**	4.8 ±0 **cd**	4.5 ±0.1 **bc**	7.39 ±0.97 **ab**	10.14 ±1.47 **bc**
Cu-NPs	1120 ±685 **a**	1830 ±611 **a**	5.9 ±0 **f**	5.8 ±0.1 **ef**	4.56 ±1.45 **a**	14.49 ±1 **c**
$CuSO_4 \cdot 5H_2O$ (10%)	0 ±0 **a**	10100 ±2310 **c**	5.2 ±0 **de**	5.5 ±0.2 **def**	nd	nd

521

522

523 **Table 2. Analyses of EXAFS spectra.** The Cu K-edge EXAFS model best fit parameters
524 of the nearest coordination shells around the Cu atoms in a) Cu-oxalate standard and b)
525 blue Cu complex, produced by fungus *Botrytis cinerea* growing on CuO-NPs.

a) Cu-oxalate	**Cu neighbor**	**N**	**R (Å)**	**σ^2 (Å^2)**
	O	4.0	1.94 (1)	0.004 (1)
	O	2.0	2.64 (3)	0.004 (3)
	C	2.0	2.7 (5)	0.025 (9)
	C	2.0	2.8 (2)	0.008 (6)
	C	2.0	3.1 (1)	0.008 (6)

b) Blue complex	**Cu neighbor**	**N**	**R (Å)**	**σ^2 (Å^2)**
	O	4.0	1.97 (1)	0.004 (1)
	O	2.0	2.66 (3)	0.003 (2)
	C	2.0	2.6 (1)	0.009 (6)
	C	2.0	3.0 (6)	0.025 (9)
	C	2.0	3.1 (1)	0.009 (6)

526 N = number of nearest Cu neighbor atoms, R = distance, σ^2 = Debye-Waller factor. The
527 uncertainty of the last digit is given in parentheses.

528

Figure captions

Figure 1. a) Water content in fungal mycelia (%), b) biomass production and, c) MDA in fresh mycelia. Data are presented as mycelia dry biomass of fungi (means ±SE; n=3) and MDA concentrations in fresh fungi (means ±SE; n=4) grown in suspensions of CuO-MPs, CuO-NPs, Cu-NPs and $CuSO_4 \cdot 5H_2O$ (1 and 10%) for 2 weeks. Different letters above the columns represent statistically significant differences (Tukey test, performed for both fungal species together; $p<0.05$); nd = not determined.

Figure 2. Appearance of *A. alternata* (top left) and *B. cinerea* (center, top right) mycelia on different copper treatments: control, CuO-MPs, CuO-NPs, Cu-NPs and $CuSO_4 \cdot 5H_2O$ (10%). Photographs were taken 12 weeks after inoculation, from top and bottom of the Petri dishes. The Cu distribution is presented as Cu concentrations (mg cm^{-2}) in half-cm distances from the center of the inoculated Petri dishes (T-transparent zone, B-blue Cu complex, F-fungi; mind differences in the scales).

Figure 3. The LA-ICP-MS Cu distribution patterns in *A. alternata* and *B. cinerea* mycelia (O-old, Y-young) grown in control, $CuSO_4 \cdot 5H_2O$ (1%), CuO-MPs, CuO-NPs and Cu-NPs..

Figure 4. Siderophores assessment on CAS agar after 2 days of post-inoculation: a) *A. alternata* mycelia with yellow halos and b) *B. cinerea* mycelia with purple halos.

Figure 5. Fourier transform magnitude of k^3-weighted copper K-edge EXAFS spectra measured on the Cu complexes (blue compound, produced by the fungus *Botrytis cinerea* growing on CuO-NPs), and on reference Cu-oxalate (solid lines), and best fit EXAFS model (dotted line) based on crystal structure data of Cu-oxalate.

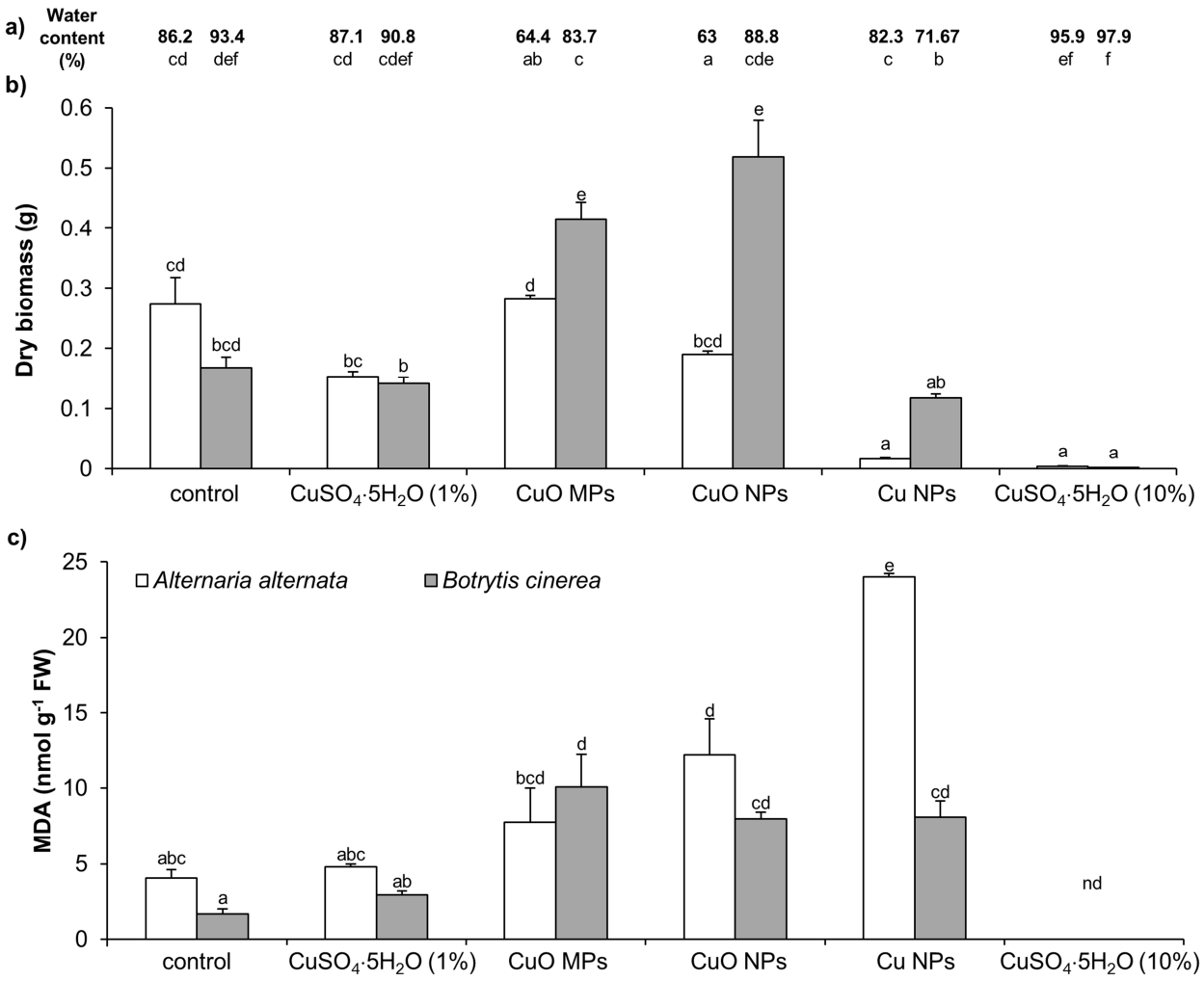
a)
Water content (%)
86.2 93.4
cd def
87.1 90.8
cd cdef
64.4 83.7
ab c
63 88.8
a cde
82.3 71.67
c b
95.9 97.9
ef f
b)
Dry biomass (g)
0.6
0.5
0.4
0.3
0.2
0.1
0
cd
bcd
bc
b
d
e
bcd
e
a
ab
a
a
control
CuSO4·5H2O (1%)
CuO MPs
CuO NPs
Cu NPs
CuSO4·5H2O (10%)
c)
Alternaria alternata
Botrytis cinerea
MDA (nmol g-1 FW)
25
20
15
10
5
0
abc
a
abc
ab
bcd
d
d
cd
e
cd
nd
control
CuSO4·5H2O (1%)
CuO MPs
CuO NPs
Cu NPs
CuSO4·5H2O (10%)

Figure 1.

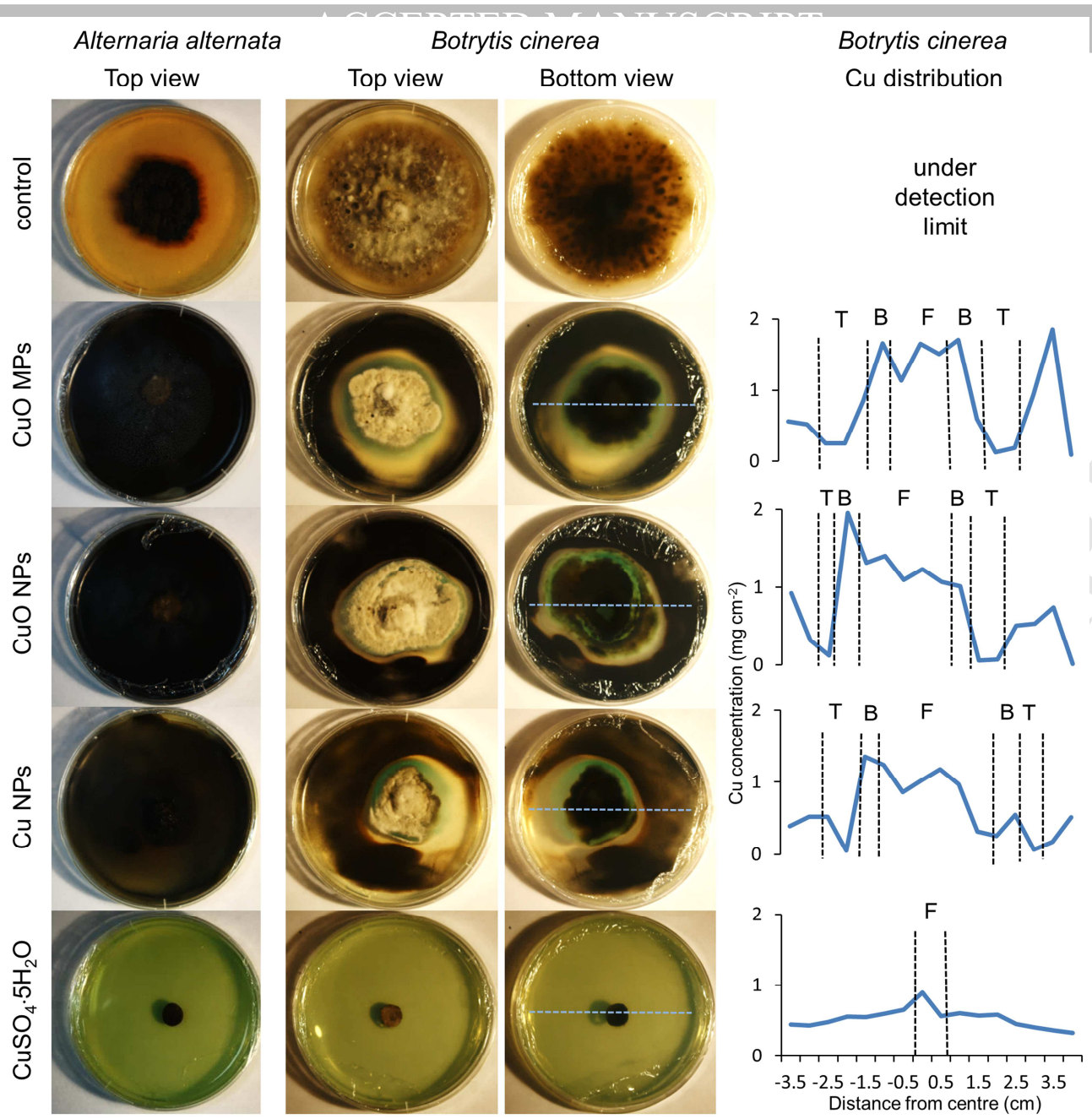

Figure 2.

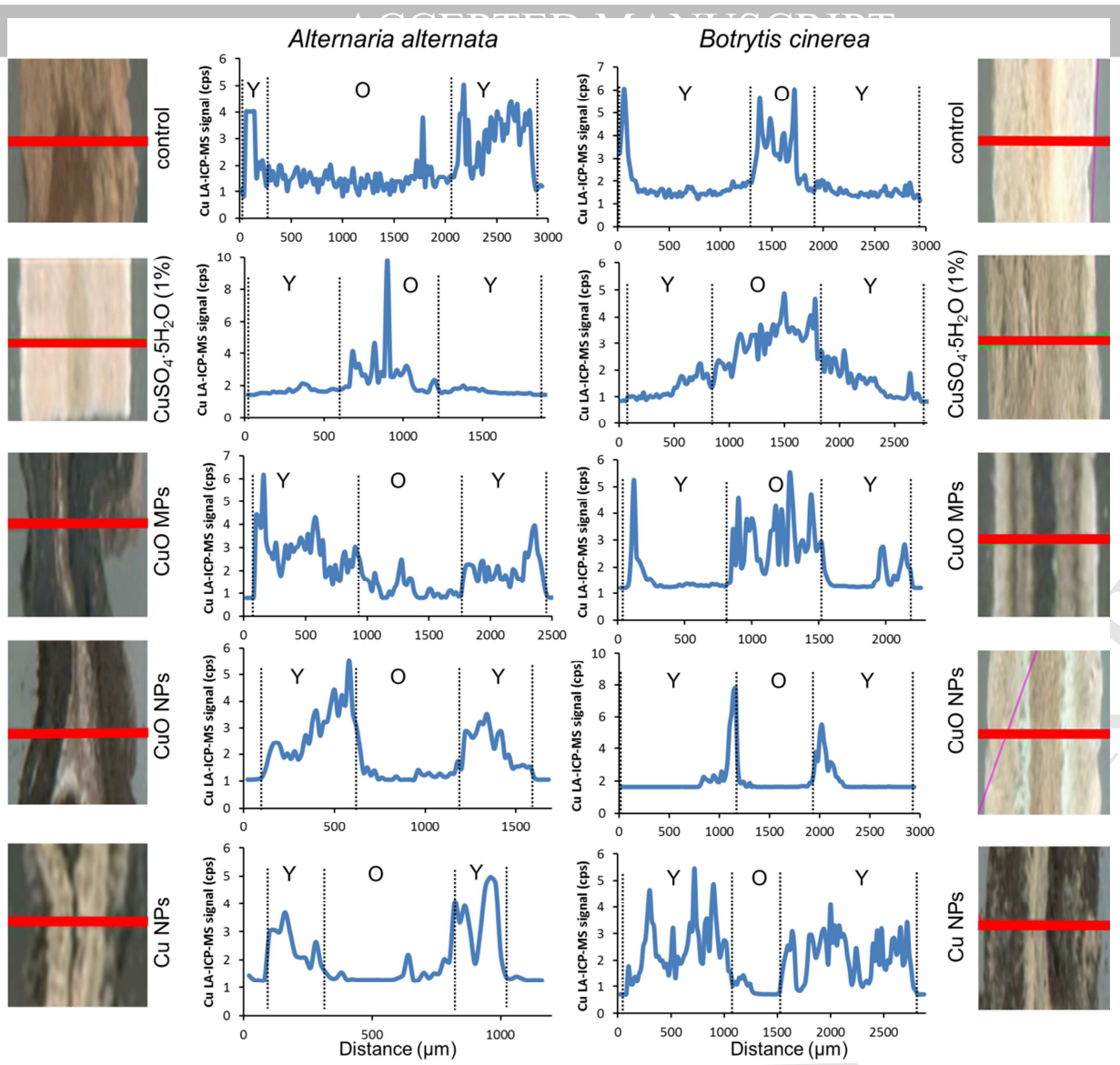

560

561 **Figure 3.**

562

563

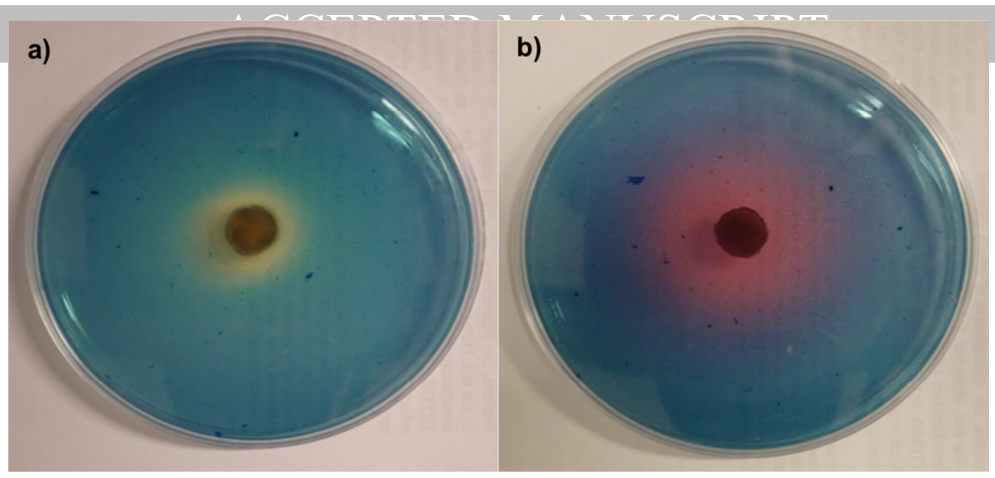

564

565 **Figure 4.**

566

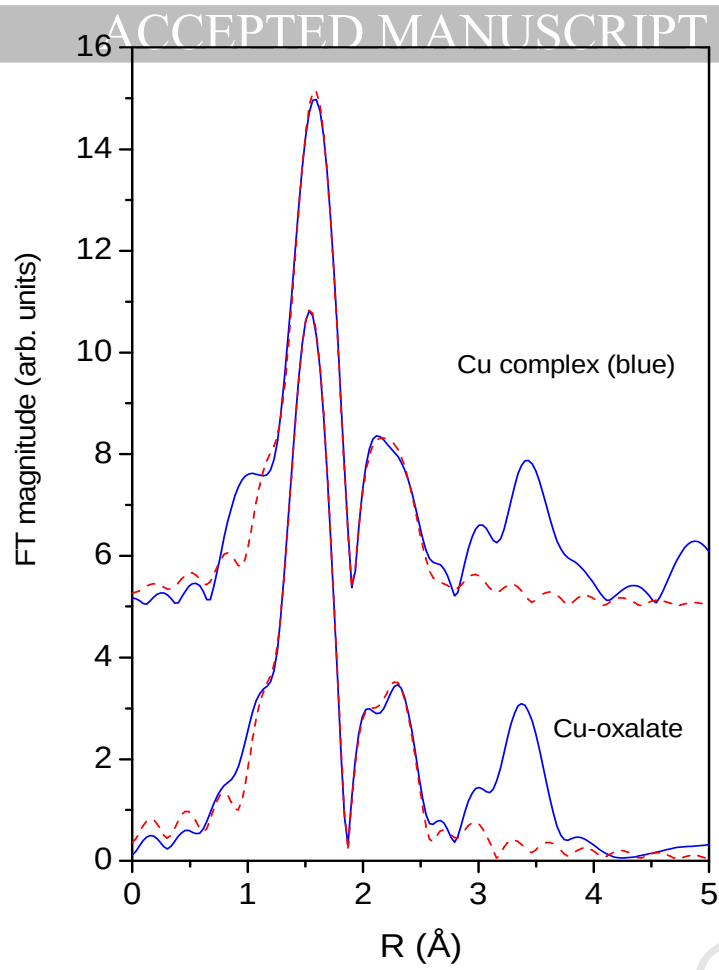

Figure 5.

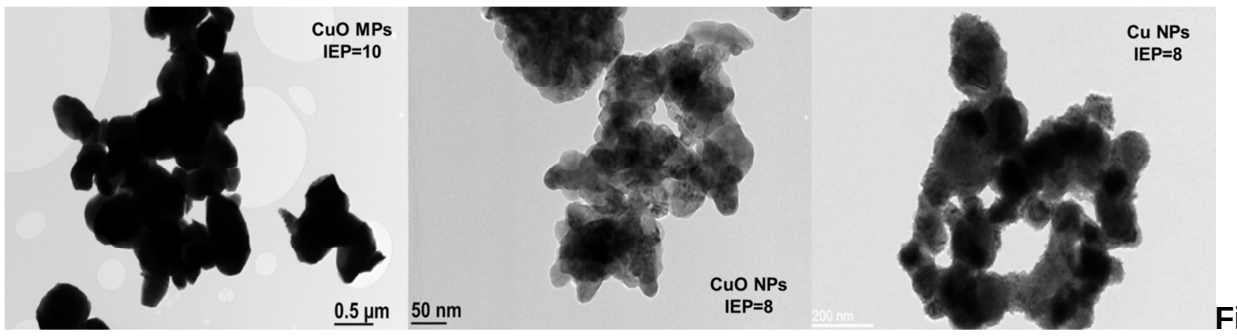

571 **Fig. A. Characteristics of different Cu-based particles.** TEM micrographs of CuO-MPs,
572 CuO-NPs and Cu-NPs revealing their size and shape. Information on isoelectric point (IEP)
573 is also given.

574

575

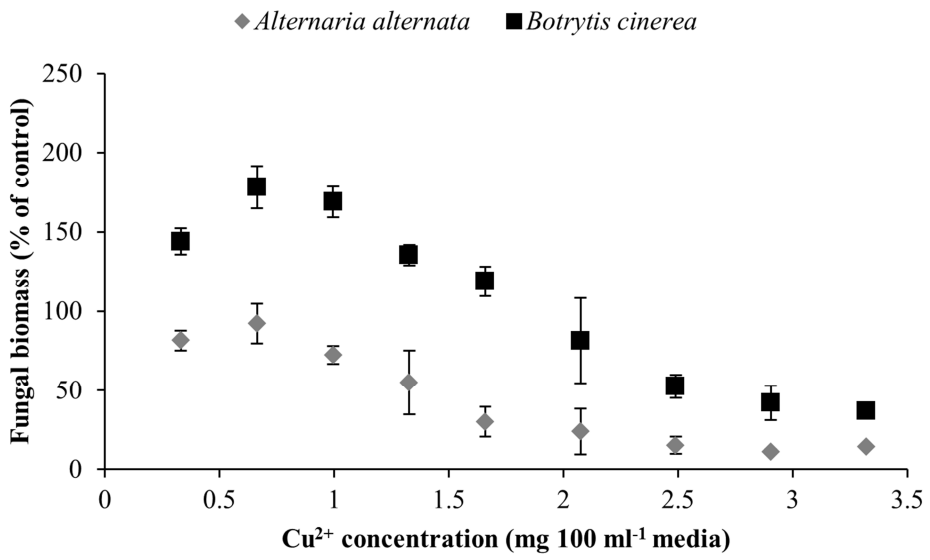

576

577 **Fig. B. Biomass production of fungi exposed to different concentrations of Cu^{2+}.**

578

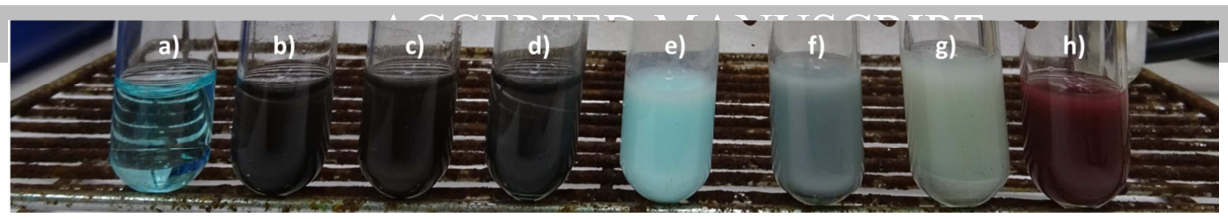

Fig. C. Solubility of different Cu compounds. Solvents used were Milli Q water and 1M oxalic acid. In each test tube 5 ml of the solvent was put together with 500 mg of different Cu-based particles. The photography was taken after 24 hours. From left to right: a) $CuSO_4.5H_2O$ in dH_2O, b) CuO-MPs in dH_2O,c) CuO-NPs in dH_2O, d) Cu-NPs in dH_2O, e) $CuSO_4.5H_2O$ in oxalic acid, f) CuO-MPs in oxalic acid, g) CuO-NPs in oxalic acid and h) Cu-NPs in oxalic acid.

Highlights

- *B cinerea* is more resistant/ tolerant to CuO and Cu NPs than *A. alternata*
- *B. cinerea* excretes oxalic acid and catechol-type siderophores
- *B. cinerea* is able to biotransform CuO and Cu NPs to Cu-oxalate
- CuO and Cu NPs may not be efficient in treating *B. cinerea* based plant diseases
- *B. cinerea* could be used for cleaning environment contaminated with CuO and Cu NPs